Icarus 243 (2014) 104–110

Contents lists available at ScienceDirect

Icarus

journal homepage: www.elsevier.com/locate/icarus

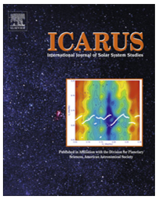

Evidence for longitudinal variability of ethane ice on the surface of Pluto

B.J. Holler [a,*,1], L.A. Young [b,1], W.M. Grundy [c,1], C.B. Olkin [b,1], J.C. Cook [b]

[a] *Laboratory for Atmospheric and Space Physics, University of Colorado at Boulder, 1234 Innovation Dr., Boulder, CO 80303, United States*
[b] *Southwest Research Institute, 1050 Walnut St. #300, Boulder, CO 80302, United States*
[c] *Lowell Observatory, 1400 W. Mars Hill Rd., Flagstaff, AZ 86001, United States*

ARTICLE INFO

Article history:
Received 6 June 2014
Revised 8 September 2014
Accepted 9 September 2014
Available online 16 September 2014

Keywords:
Pluto, surface
Ices, IR spectroscopy
Photochemistry
Pluto
Spectroscopy

ABSTRACT

We present the results of an investigation using near-infrared spectra of Pluto taken on 72 separate nights using SpeX/IRTF. These data were obtained between 2001 and 2013 at various sub-observer longitudes. The aim of this work was to confirm the presence of ethane ice and to determine any longitudinal trends on the surface of Pluto. We computed models of the continuum near the 2.405 μm band using Hapke theory and calculated an equivalent width of the ethane absorption feature for six evenly-spaced longitude bins and a grand average spectrum. The 2.405 μm band on Pluto was detected at the 7.5-σ level from the grand average spectrum. Additionally, the band was found to vary longitudinally with the highest absorption occurring in the N_2-rich region and the lowest absorption occurring in the visibly dark region. The longitudinal variability of ^{12}CO does not match that of the 2.405 μm band, suggesting a minimal contribution to the band by ^{13}CO. We argue for ethane production in the atmosphere and present a theory of volatile transport to explain the observed longitudinal trend.

1. Introduction

Almost 85 years have passed since the discovery of Pluto, yet its surface characteristics are still not fully understood. The primary surface ice components are N_2, CH_4, and CO (Cruikshank et al., 1997). The presence of these volatile ices is elegantly explained by comparing Pluto's surface temperature (~40 K; Tryka et al., 1994; Lellouch et al., 2000, 2011) and diameter (~2368 km; Lellouch et al., in press) to the volatile loss curves of N_2, CH_4, and CO (Schaller and Brown, 2007). Pluto is sufficiently large and cold to retain these species over the age of the Solar System and is able to support an atmosphere of N_2, CH_4, and CO (e.g.: Elliot et al., 2007). However, these volatile ices vary both with Pluto longitude and time (Grundy et al., 2013, hereafter referred to as G13; Grundy et al., 2014, hereafter referred to as G14). These variations are most likely due to changes in illumination across Pluto's surface as it orbits the Sun, allowing for sublimation of volatiles and subsequent transport, or to changes in viewing geometry.

In addition to Pluto's changing axial orientation with respect to the Sun and Earth, chemical processes are altering the composition of the surface. Extreme-UV photons and cosmic rays interact with molecules in the atmosphere, on the surface, and in some cases can penetrate deeper into the ice. In particular, CH_4 molecules may undergo photolysis or radiolysis to be converted into other hydrocarbon products such as acetylene (C_2H_2), ethylene (C_2H_4), ethane (C_2H_6), and propane (C_3H_8) (Lara et al., 1997; Krasnopolsky and Cruikshank, 1999; Moore and Hudson, 2003). From Fig. 32 in Fray and Schmitt (2009), the sublimation pressures (at 40 K) of N_2 (~100 μbar), CO (~10 μbar), and CH_4 (~0.01 μbar) are much higher than those of acetylene, ethylene, and ethane (≪0.001 μbar). Non-methane hydrocarbon species shall henceforth be referred to as non-volatiles since their sublimation pressures are negligible at 40 K.

A simple calculation of the flux of Lyman-α photons reaching the surface of Pluto can answer the question of where photochemistry takes place: On the surface or in the atmosphere? The flux of photons ($F = F_0 e^{-\sigma N}$) hitting Pluto's surface depends on the photon flux at Pluto's orbital distance of 30 AU ($F_0 = 3 \times 10^8\ \mathrm{cm^{-2}\ s^{-1}}$; Madey et al., 2002), the UV cross section of CH_4 at 120 nm ($\sigma = 1.8 \times 10^{-17}\ \mathrm{cm^2}$; Chen and Wu, 2004), and the column density of CH_4 ($N = 1.75 \times 10^{19}\ \mathrm{cm^{-2}}$; Lellouch et al., 2009). This calculation yields a flux of Lyman-α photons on the order of $10^{-129}\ \mathrm{cm^{-2}\ s^{-1}}$, a number that is effectively zero. If Pluto's atmosphere collapses, this calculation is no longer valid. Thus we assume photochemical products such as ethane are mainly formed in the atmosphere (Lara et al., 1997; Krasnopolsky and Cruikshank,

---

[*] Corresponding author.
E-mail address: bryan.holler@colorado.edu (B.J. Holler).

[1] Remote observer at the Infrared Telescope Facility, which is operated by the University of Hawaii under, Cooperative Agreement #NNX-08AE38A with the National Aeronautics and Space Administration, Science, Mission Directorate, Planetary Astronomy Program.

http://dx.doi.org/10.1016/j.icarus.2014.09.013

1999) and the descent time is long enough that horizontal winds may transport the products a great distance away from the region of origin before precipitating onto the surface (Mark Bullock, private communication). This will result in a uniform surface distribution of photochemical products regardless of whether the atmospheric CH_4 is uniform (Lellouch et al., in press) or not (Cook et al., 2013). These non-volatile ices may subsequently be covered over time by deposition of volatiles onto the surface.

Sasaki et al. (2005) performed a search for acetylene, ethylene, ethane, and propane ices on Pluto in the *L* band (3.0–4.0 μm) but the results were inconclusive. DeMeo et al. (2010) identified weak ethane absorption bands at 2.274, 2.405, 2.457, and 2.461 μm in the *K* band and constrained pure ethane to <10%. The 2.405 μm band coincides with an absorption band of ^{13}CO, an isotopologue of the more abundant ^{12}CO (Cruikshank et al., 2006). DeMeo et al. (2010) argue that the 2.405 μm band is too deep compared to the 2.457 and 2.461 μm bands, and therefore ^{13}CO must contribute to the depth of the 2.405 μm band. However, individual bands of a species may not reach maximum depth at the same longitude (as is the case for CH_4 on Pluto and Triton from G13 and Grundy et al., 2010, respectively). Additionally, Cruikshank et al. (2006) argue, based on currently unpublished CO laboratory data, that the contribution of ^{13}CO is negligible and that the 2.405 μm feature is almost entirely due to ethane absorption. This issue will be addressed more thoroughly in Section 5. In the same manner as DeMeo et al. (2010), Merlin et al. (2010) find less pure ethane ice on Pluto's surface (5%) in favor of more heavily radiation-processed tholins (20%). They also present an ethane life cycle theory where the surface of Pluto is effectively shielded from radiation and cosmic rays by the atmosphere during perihelion and covered in N_2 ice during aphelion. They indicate a preference for ethane creation either on methane-rich surface ice patches during aphelion or within the atmosphere during perihelion. See Fig. 1 for ethane bands relevant to this work and Table 1 in Hudson et al. (2009) for a full description of ethane absorption bands seen in the infrared.

2. Observations

The combined Pluto/Charon spectra analyzed in this investigation were obtained on 72 nights from 2001 to 2013 using the SpeX infrared spectrograph on the 3-m Infrared Telescope Facility (IRTF) (Rayner et al., 1998, 2003). The reader is referred to Table 1 in G13 for observational circumstances of the first 65 nights (2001–2012), and Table 1 in G14 for the observational circumstances of the later seven nights (2013). The observed wavelength range covered 0.8–2.43 μm using slit widths of 0.3″ ($\lambda/\Delta\lambda \sim 1600$–1900) and 0.5″ ($\lambda/\Delta\lambda \sim 1200$); the slit is 15″ in length. Pluto itself subtends 0.1″ while the maximum separation between Pluto and Charon is 1″, too small for SpeX to routinely spatially resolve the two bodies. Charon accounts for 20.8% of the total reflecting area in the Pluto system. However, Charon contributes less than 20.8% of the light in a combined Pluto/Charon spectrum since Charon's albedo is wavelength-dependent and generally lower than Pluto's between 0.8 and 2.43 μm (Douté et al., 1999). Spectra were obtained with the slit rotation parallel to the imaginary line connecting Pluto and Charon so that the fraction of light from Charon was independent of slit width, seeing, or guiding accuracy. This eliminated the need to quantify Charon's contribution for each individual spectrum taken throughout a given night. We included Charon's contribution when performing spectral modeling. Pluto's minor satellites Nix, Styx, Kerberos, and Hydra are so small as to be negligible in this analysis (Weaver et al., 2006; Showalter et al., 2011, 2012). For a more thorough description of our observing process, the reader is again referred to G13 and G14.

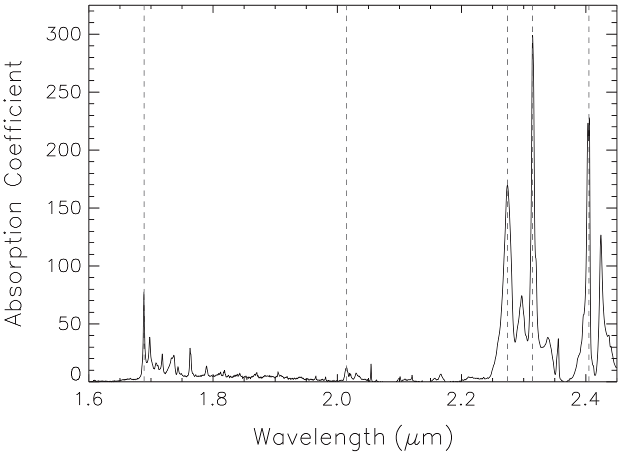

Fig. 1. Absorption coefficients for pure ethane (C_2H_6) at 21 K (adapted from Quirico and Schmitt, 1997a). Dashed gray lines mark the positions of ethane bands of interest in the range 1.6–2.45 μm. From left to right: 1.689, 2.015, 2.274, 2.314, and 2.405 μm. The spectral range of IRTF/SpeX is 0.8–2.43 μm.

3. Analysis

The raw spectra were reduced as described in G13. The reduced spectra analyzed in this investigation can be found as Supplementary material accompanying this paper and at http://www2.lowell.edu/users/grundy/abstracts/2014.IRTF-Pluto.html. A weighted average was performed on the albedo values within each wavelength interval; each value was weighted according to its uncertainty, with more accurate measurements given larger weighting factors. The resulting grand average spectrum, calculated from 72 individual spectra and covering 0.8–2.43 μm, has a spectral resolution of ~1100 and a signal-to-noise ratio (SNR) of 155 and is seen in Fig. 2. The SNR was calculated by fitting a portion of the spectrum (2.38–2.40 μm) to a cubic polynomial and evaluating the scatter of the data points with respect to the fit. This region was chosen to calculate the SNR because it not only was a good fit to a cubic but also comprised a large portion of the region included in the later analysis. The 72 spectra were then sorted into six longitude bins covering the 60° intervals described in Table 1. The spectra in each longitude bin were averaged in the same manner as the grand average. The bin ranges were chosen based on the spectral characteristics described in Fig. 3. Bins 1 and 2 roughly match the section observed to be dark in Pluto's visible light curve (Buie et al., 2010a,b); this region is most likely dominated by low-albedo tholins, but this has yet to be confirmed. Bins 3 and 4 roughly correspond to a region of Pluto dominated by N_2 ice with a peak in absorption of CO, two species found to be spatially concurrent on Pluto (G13); the visible light curve also peaks in this region (Buie et al., 2010a,b). Bins 5 and 6 cover the third of Pluto dominated by CH_4 ice.

The goal of this investigation was to determine how ethane abundance varies as a function of longitude across Pluto's surface. Our analysis focused on the 2.405 μm band. Other potential ethane bands within the range of the data (0.8–2.43 μm) at 1.689, 2.015, 2.274, and 2.314 μm suffered from confusion by strong CH_4 absorption bands or telluric absorption. More bands exist at 2.457 and 2.461 μm but fell outside of the data range. We made use of code based on Hapke theory (e.g.: Hapke, 2012) to construct synthetic spectra that modeled the region near the 2.405 μm band. For convenience, these models will be referred to henceforth as ethane-absent continuum models. They are not spectrally flat, but instead are models assuming no ethane present on Pluto's